Discovery of a multi-functional biocatalyst for asymmetric conjugate reduction-reductive amination

Nicholas Turner (Nicholas.Turner@manchester.ac.uk)
University of Manchester https://orcid.org/0000-0002-8708-0781

Thomas Thorpe
University of Manchester

James Marshall
University of Manchester

Vanessa Harawa
University of Manchester

Rebecca Ruscoe
University of Manchester

Anibal Cuetos
University of York

James Finnigan
Prozomix

Antonio Angelastro
University of Manchester

Fabio Parmeggiani
University of Manchester

Simon Charnock
Prozomix

Roger Howard
Pfizer Worldwide Research and Development

Rajesh Kumar
Pfizer Worldwide Research and Development

David Daniels
Pfizer Worldwide Research and Development

Gideon Grogan
University of York

Physical Sciences - Article

Keywords: Chemical Synthesis, Catalytic Systems, Enantioenriched Amine Diastereomers, α,β-unsaturated Carbonyls, Stereocentre Control

Posted Date: July 12th, 2021

DOI: https://doi.org/10.21203/rs.3.rs-640129/v1

Version of Record: A version of this preprint was published at Nature on April 6th, 2022. See the published version at https://doi.org/10.1038/s41586-022-04458-x.

Abstract

A major challenge in chemical synthesis is to develop catalytic systems that convert simple molecules to complex high-value products. Often these valuable compounds must be manufactured asymmetrically, as their biochemical properties can differ based on the chirality of the molecule. Of great interest are enantioenriched amine diastereomers, which are prevalent in pharmaceuticals and agrochemicals,[1] yet their preparation often relies on low-efficiency multi-step synthesis.[2] Herein, we report the discovery and characterisation of a multi-functional biocatalyst, which operates using a previously unreported conjugate reduction-reductive amination mechanism. This enzyme (pIR-120), identified within a metagenomic imine reductase (IRED) collection[3] and originating from an unclassified Pseudomonas species, possesses an unusual active site architecture that facilitates an amine-activated conjugate alkene reduction followed by reductive amination. This enzyme enables the coupling of a broad selection of α,β-unsaturated carbonyls with amines for the efficient preparation of enantioenriched amine diastereomers. Moreover, employing a racemic substrate partner or conjugated dienyl-ketone provides a means of controlling additional stereocentres using the single catalyst. Mechanistic and structural studies have been carried out to delineate the order of individual steps catalysed by pIR-120 which have led to a proposal for the overall catalytic cycle. This work shows that the IRED family can serve as a platform for facilitating the discovery of further enzymatic activities for application in synthetic biology and organic synthesis.

Main

The prevalence of chiral amines in active pharmaceutical ingredients (APIs) and other high value chemicals[1] has led to an overarching goal in organic synthesis to develop efficient new catalytic methods for their preparation.[4] In this context, reductive amination (RA) is one of the most widely used and powerful methodologies in medicinal chemistry, enabling efficient formation of C-N bonds through the reductive coupling of carbonyls and amines.[2,5] The development of effective catalysts for asymmetric RA continues to be explored, including those based on metallo-,[6,7] organo-[8] and biocatalysis.[3,9–11] Furthermore, valuable amino-compounds often contain multiple stereogenic centres (Fig. 1a), however total control of their asymmetry is more challenging, resulting in less efficient multistep syntheses[12] or more complex tandem catalysis systems.[13,14] Whilst multi-enzyme systems are highly amenable to these biomimetic tandem processes (Fig. 1b), difficulties in their assembly arise from incompatibilities of their reaction medium and reaction rates, which can lead to by-product formation and intricate reaction setup.[15] To address these issues and achieve the desired reaction metrics, significant protein engineering is often required on each enzyme component.[16] Discovery of a single enzyme that can control multiple stereocentres through a RA-like process would be highly desirable and enable efficient synthesis of valuable amine diastereomers using a one-pot, one-catalyst system (Fig. 1c).

Nicotinamide-dependent enzymes are versatile biocatalysts for both asymmetric conjugate reduction (CR)[17,18] and reductive amination (RA).[9,10,19,20] For RA, imine reductases (IREDs) have emerged as

attractive catalysts since they possess broad substrate scope and can be engineered for industrial application.[21,22] IREDs are characterised as chemoselective for the reduction of C=N bonds[23–25] although under exceptional circumstances they can reduce C=O bonds of activated carbonyl species.[26] Furthermore, we recently demonstrated that IREDs could be combined with ene-reductases (EREDs) in a one-pot process to reduce both the C=C and C=N bonds of cyclic enimines (*α,β*-unsaturated imines).[27] We speculated that if an IRED could catalyse both of these steps, in a similar fashion to recently reported biosynthetic oxidoreductases,[28,29] this biocatalyst could be applied to the CR-RA of *α,β*-unsaturated carbonyls and allow access to enantioenriched amine diastereomers (Fig. 1c).

In pursuit of this activity, we screened both reported[9,25,30–32] and our recently established (meta)genomic IREDs[3,33] for the complete reduction of cyclic enimine **I** to amine **II** (Fig. 1d and Supplementary Table. ST1). Amongst the 389 IREDs screened, we observed that 262 catalysed reduction of **I**, with the majority behaving conventionally, *i.e.* reducing the C=N bond only (206 enzymes, 53%). Gratifyingly, a smaller subset of IREDs were able to catalyse the reduction of both the C=C and C=N bonds of **I** to the diastereomerically enriched product **II** (44 enzymes, 11%). Furthermore, in a complementary fashion, some IREDs reduced solely the C=C bond (12 enzymes, 3%). Mapping the reaction profiles against genetic sequence indicated localised sequence-activity correlation only (Extended Data Fig. ED1). One particular metagenomic enzyme, likely originating from an unclassified *Pseudomonas* species (pIR-120, Fig. 1d), exhibited excellent full reduction of **I** to **II**, and hence this enzyme was selected for further study.

pIR-120 was next examined for the ability to catalyse CR-RA of cyclohex-2-enone **1** with allylamine **a**, monitoring for potential reduced and coupled products **1a**, **1'**, **1'a** including aza-conjugate addition. The reaction proceeded with high conversion, forming predominately CR-RA product **1'a** and CR product **1'** without concomitant generation of direct RA product **1a**. In the absence of pIR-120, or the nicotinamide cosubstrate regeneration system, no reduction products could be detected. Optimisation of the buffer type, pH as well as co-solvent (Extended Data Fig. ED2) increased the conversion to **1'a** and could be scaled-up using 20 eq. of **a** yielding the hydrochloride salt in 69% yield (Fig. 1e).

We explored the substrate scope of pIR-120 using the optimised reaction conditions (Fig. 2). Preliminary experiments revealed that cyclopropylamine **b** displayed high activity with *α,β*-unsaturated carbonyls and hence was screened against a large panel of substrate partners **1**-**23** (for a full list of substrates see Supplementary Fig. SF4). pIR-120 exhibited a broad substrate scope, accepting enals as well as acyclic and cyclic enones, yielding CR and mono-RA products. Generally, unhindered enals and enones could be transformed with high chemoselectivity to the corresponding saturated amines. This trend is observed by comparing the reaction profiles of increasingly hindered C_2-substituted but-2-enals **3**-**5** or decreasingly hindered amine donors **a**-**c** with cinnamaldehyde **6.**

Cyclic enones with various ring sizes were all accepted by pIR-120, with 5- and 6-membered, **1** and **10,** affording good conversion to the corresponding saturated amine products **1'b** or **10'b** without direct RA products **1b** or **10b**. 2-, 3- and 4,4'-methyl substituted cycloalkyl-2-enones **12-15** were also accepted by the enzyme, with 3-substituted **12** and **15** offering high conversion, chemo- and stereoselectivity to the

corresponding CR-RA products **12'b** and **15'b**. C_3-elaboration of the cyclohex-2-enone scaffold **15**-**22** was generally well tolerated, offering excellent conversion, chemo-, enantio- and (*trans*)-diastereoselectivity to the corresponding *N*-substituted cyclohexylamines **15'b, 16'b, 18'b** and **20'b**. This included sterically crowded enone **20** as well as functionalised derivative **18** that provides a handle for subsequent downstream chemistry.

A broad selection of amine partners was explored using 3-methyl-cyclohexenone **15** as substrate partner. Excellent conversion, chemo-, enantio- and diastereoselectivities were observed for small linear primary amines **a**-**c**, **e**-**h**. Notably, functionalised products from amines **a**, **e**, **g**, **h** could be formed efficiently as well as the secondary amine pyrrolidine **i**.

We were also keen to see if CR-RA products with additional stereocentres could be synthesised. (*R*) or (*S*)-3-fluoropyrrolidine **j** could be coupled efficiently with 3-methylcyclohexenone **15**, affording (*cis*)-**15'j** with high chemo- and diastereoselectivity (see Supplementary Discussion for details on the use of *rac*-**j**). Note that the introduction of an F-substituent on the pyrrolidine ring led to a change in relative stereochemistry across the cyclohexylamine ring. Furthermore, CR-RA of cyclopropylamine **b** with racemic enone **23** demonstrated that the single catalyst could control three stereocentres on cyclohexylamine ring **23'b**, offering excellent enantioselectivity as well as good chemo- and diastereoselectivity.

To assess the synthetic applicability of the pIR-120-catalysed CR-RA, preparative-scale syntheses were performed using **15** partnered with **a**, **b** or **i** as well as **16** combined with **b** forming **15'a**, **15'b**, **15'i**, and **16'b** as the hydrochloride salts in 81%, 77%, 60% and 72% isolated yield respectively (Extended Data Fig. ED3). The former example could be intensified to 50 mM **15** and 250 mM **b** substrate loadings, affording **15'b** in 64% isolated yield at a scale of 1.0 mmol (110 mg, TTN = 640).

We next carried out mechanistic investigations to further characterise pIR-120 and identify any intermediates formed during CR-RA. Isotopic labelling experiments, using the *in situ* generated deuterated nicotinamide cosubstrate from D-glucose-1-d_1, yielded 1,3-d_2-**15'b** from **15** and **b** as the hydrochloride salt (Fig. 3a, 75% isolated yield, 91% 2D incorporation). This isotopic labelling pattern suggests pIR-120 mediates asymmetric hydride transfer at both C1 and C3 of the unsaturated carbonyl substrate via a nicotinamide cosubstrate.

A time course study is consistent with a stepwise CR-RA double hydride transfer mechanism in which firstly enone **15** undergoes CR to an intermediate enantioenriched ketone (*R*)-**15'**, before RA of the intermediate to the final product (1*R*,3*R*)-**15'b** (Extended Data Fig. ED4). Importantly, no direct RA product **15b**, a potential alternative intermediate**,** was observed during the time course, suggesting that the reaction proceeds via ketone **15'** only. Furthermore, whilst **15b** was inert to redox activity with pIR-120 and cosubstrates (Fig. 3b), ketone (*R*)-**15'** undergoes RA with **b** (Fig. 3c), indicating **15'** as the sole reaction intermediate.

Knowledge of the CR-RA intermediate enabled determination of the factors controlling stereochemistry at the C2 of the *α,β*-unsaturated carbonyl through the comparison of the CR-RA of 2-methylcyclohex-2-enone **14** with corresponding RA of C2-racemic (rac)-**14'** intermediate. The product of both substrates (1*S*,2*R*)-**14'b** was formed in comparable dr and ee suggesting that C2 stereochemistry is likely controlled *via* a kinetic resolution process in the RA step (Extended Data Fig. ED5).

We were also keen to probe the enzyme-substrate complex formed during the CR step. Omitting any amine donor from the reaction yielded no product of either CR or RA (Fig. 3d), suggesting that the IRED-catalysed reaction explicitly requires the presence of an amine in the catalytic cycle. Furthermore, no activity was observed when combining either enone **15** with tertiary amine donor triethylamine **k** or unsaturated ester methyl cyclohex-1-ene-1-carboxylate and cyclopropylamine **b**, suggesting that pIR-120-catalysed CR likely occurs *via* an enimine-NAD(P)H-enzyme complex, reminiscent of organocatalytic CR systems.[34] To the best of our knowledge this is the first example of an enzyme that achieves CR by this type of enimine intermediate.

The multiple activities of pIR-120 prompted us to study its structure using X-ray crystallography. Crystals of pIR-120 in complex with $NADP^+$ were obtained in the $P2_1$ space group with two molecules in the asymmetric unit, forming the now familiar domain swapping dimeric fold observed in for the IRED family (Fig. 3e).[9,35] A comparison of the monomer structure with others in the Protein DataBank using the DALI server[36] revealed that the closest existing IRED structures in the database were those from *Streptosporangium roseum* (PDB code 5OCM; 30% seq id; rmsd 1.6 Å over 286 Ca atoms),[37] *Aspergillus oryzae* (5G6S; 30%; 1.6 Å)[9] and *Stackebrandtia nassauensis* (6JIT, 30%; 2.0 Å). The most striking differences with other IRED folds having structures in the database were observed in the active site (Fig. 3f).

pIR-120 possesses a tyrosine residue, Y177 at the top of the ceiling of the active site as drawn, in common with other IREDs, such as those from *Streptomyces* sp. GF3546 (4OQY),[38] *Bacillus cereus* (4D3F),[39] and *Nocardopsis halophila* (4D3S)[38], which have been shown to display (*S*)-stereoselectivity for the reduction of the model imine compound 2-methyl pyrroline. In common with those enzymes, in pIR-120 Y177 forms a hydrogen bond with the hydroxyl group of a side-chain, in this case threonine T101, which in turn H-bonds to the 2'-hydroxyl of the ribose in $NADP^+$. However, pIR-120 also possesses an additional tyrosine residue Y181 that also points into the active site towards the cosubstrate binding cleft, which is a hydrophobic leucine in both 5OCM and 6JIT. The active site also features a number of cyclic and hydrophobic amino acid side-chains F185, Y269, H245 and A240 with Y129 at the rear and V244 at the front, that form a closed cavity which has been previously observed to be suitable for binding, especially of planar cyclic imines in IRED structures.[9,40]

A model of the enzyme active site in complex with the enimine formed by condensation of **15** with **b** was constructed using AutoDock Vina (Fig. 3f).[41] In the top pose, the model suggests that the closest atom to the C4 of the pyridinium ring of the cosubstrate, suitable for acceptance of a hydride, is the prochiral

carbon atom of the C=C bond. Delivery of a hydride to this atom as shown in the model would give the experimentally observed (*R*)-configuration at this centre.

Based on our structural and mechanistic investigation the following dual pIR-120 catalytic cycle is proposed for productive CR-RA (Fig. 4a). First, the nicotinamide cosubstrate and condensation product of *α*,*β*-unsaturated carbonyl **V** and amine form an active-site enimine-NAD(P)H-pIR-120 complex **VI**. Where substrate orientation kinetically favours the C4 of the enimine orientated toward the nicotinamide hydride, CR yields the stereoenriched 1-enamine-$NAD(P)^+$-pIR-120 complex **VII**. Following this, the oxidised cosubstrate and prochiral 1-enamine are expelled from the enzyme, with the latter being hydrolysed in solution to form the stereoenriched carbonyl **VIII**. A further NAD(P)H cosubstrate binds to the enzyme together with the condensation product of the previously released carbonyl **VIII** and amine to form complex **IX** which undergoes the expected IRED-catalysed RA,[9] yielding the stereoenriched final product **X**.

Finally, we sought to further extend the enzyme catalysed CR-RA by employing a conjugated dienyl-ketone. Whilst **24** was susceptible to aza-conjugate addition, pIR-120-catalysed 4- and 6-electron CR-RA of *α*,*β*,*γ*,*δ*-unsaturated enone **24** in combination with cyclopropylamine **b**, affording **24'b** and (*trans*)-**24"b**=**16'b** respectively (Fig. 4b). Interestingly, 6-electron CR-RA product **24"b**=**16'b** possessed analogous diastereo- and enantioselectivity to the CR-RA of the corresponding ethyl substituted *α*,*β*-unsaturated enone **16**, suggesting that reduction of **24** proceeds by a similar pathway to that of **16**. This experiment suggests that pIR-120 could be used to establish additional stereogenic centres during the CR-RA process.

In summary, we report the discovery and characterisation of a multi-functional biocatalyst (pIR-120) that is able to catalyse CR, using a previously unreported amine activation mechanism, as well as imine reduction and RA. pIR-120 possesses broad substrate scope allowing for the stereoselective preparation of valuable amine diastereomers in a one-pot, one-catalyst reaction starting from simple prochiral starting materials. Mechanistic and structural studies reveal a multi-step process in which pIR-120, which possesses an unusual additional tyrosine residue (Y181) in its active site, first catalyses amine-activated CR of *α*,*β*-unsaturated carbonyl via a previously undescribed enimine-NAD(P)H-enzyme complex, followed by RA. This new CR-RA reaction further expands the repertoire of imine reductases and emphasises their importance in the synthesis of stereochemically defined chiral amines.

Methods

Cloning, expression and protein purification

The codon-optimised pIR-120 gene sequence (TWIST Biosciences, US, GenBank accession number MW854365) was cloned into pET-28a-(+) (Supplementary Fig. SF1) and used to transform chemically competent *E. coli* BL21 (DE3). Cultivation was performed in 400 mL Terrific Broth (TB) media (Formedium, Hunstanton, Norfolk, UK) supplemented with 35 $\mu g \cdot mL^{-1}$ kanamycin in 2 L Erlenmeyer baffled flasks. Cultures were incubated at 37 °C and shaken at 200 rpm until an optical density (OD_{600nm})

of 0.6-0.8, before gene expression was induced with isopropyl β-D-1-thiogalactopyranoside (IPTG) at a final concentration of 100 μM. Incubation was continued at 23 °C and 200 rpm for 25 h before harvesting the biomass using centrifugation. Disruption of the cells using sonication in an ice bath, then clarification by centrifugation and lyophilisation afforded powdered pIR-120 cell-free extract (CFE). To obtain purified enzyme, powdered pIR-120 CFE was resuspended, clarified by centrifugation and immobilised metal affinity chromatography (IMAC) was performed. Further purification of the protein for crystallography and control and mechanistic experiments was realised using gel filtration (GF) chromatography. For further details see Supplementary information.

Biotransformations

Typical procedure for pIR-120-catalysed CR-RA: A 200 μL reaction mixture consisting of 10 mM *α,β*-unsaturated carbonyl, 200 mM amine, 0.2 mol% pIR-120, 0.1 mg·mL^{-1} GDH, 5.0 mol% NADP^{+}, 30 mM glucose, 15% v/v DMSO, 100 mM glycine-NaOH buffer pH 9.0 were shaken at 900 rpm in 96-well microtiter plate at 30°C for 18 h before being quenched with 5.0 M NaOH (aq, 20 μL) and extracted into heptane, dichloromethane or $CDCl_3$ (2 × 200 μL). The organic fractions were combined and analysed by GC-MS before being derivatised and analysed by GC-FID over a chiral stationary phase or ^{1}H NMR. CR-RA reactions were undertaken in 2–5 replicates and could also be performed using pIR-120 CFE (4 mg·mL^{-1}) affording comparable results.

Preparative scale reactions were undertaken at 10 or 50 mM *α,β*-unsaturated carbonyl with 200-250 mM amine, 0.2 or 0.1 mol% pIR-120, 0.1 mg·mL^{-1} GDH, 1.0 mol% NADP^{+}, 30 or 150 mM glucose, 15% v/v DMSO, 100 mM glycine-NaOH buffer pH 9.0 and were shaken at 200 rpm in falcon tubes at 25°C for 24 h before being quenched with 5.0 M NaOH (aq, 0.1 × reaction volume), clarified by centrifugation and extracted into MTBE (3 × reaction volume). The organic fractions were combined, dried with $MgSO_4$ and concentrated under reduced pressure to remove excess amine substrate before acidification with 2.0 M HCl (dioxane, 2 eq) and concentration *in vacuo* to yield the amine-HCl salt which was analysed by NMR and GC-FID over a chiral stationary phase. For further details see Supplementary Information.

Declarations

Author Contributions

N.J.T., G.G., R.M.H., R.K., D.S.B.D. devised and supervised the project. F.P. and R.E.R. managed the project. T.W.T. and A.A performed mechanistic studies. T.W.T. and R.E.R carried out substrate scope reactions. A.C., T.W.T. and G.G. performed crystallographic and docking studies. T.W.T. and V.H. carried out preparative scale reactions. T.W.T., R.E.R and V.H. synthesised substrates and standards. J.R.M., S.J.C., J.D.F. performed genetic identification, cloning and bioinformatics. T.W.T. and J.R.M. produced and purified the biocatalyst, N.J.T, G.G., R.M.H., R.K, D.S.B.D., S. J. C., F.P. J.D.F., A.C, R.E.R., V.H., J.R.M. and T.W.T. wrote the manuscript and generated the figures.

Acknowledgements

T.W.T. is grateful for a CASE award from the UK Biotechnology and Biological Sciences Research Council (BBSRC) and Pfizer (BB/M011208/1). J.R.M. acknowledges a CASE award from the Industrial Biotechnology Innovation Centre (IBioIC), BBSRC, and Prozomix Ltd. A.C. was funded by grant BB/P005578/1 from the BBSRC. N.J.T. is grateful to the ERC for the award of an Advanced Grant (742987). We thank Dr Johan P. Turkenburg and Mr Sam Hart for assistance with X-ray data collection and the Diamond Light Source for access to beamline I03 under proposal number mx-9948.

Data Availability and Code Availability Statement

The data supporting the findings of this study are available within the paper and its Supplementary Information files. Sequence data has been deposited in Genbank (accession numbers MW854365, MW925135-MW925140) and the coordinate files and structure factors have been deposited in the PDB with coordinate (accession number 7A3W).

Additional Information

Supplementary Information is available for this paper. Correspondence and requests for materials should be addressed to N.J.T. Reprints and permissions information is available at www.nature.com/reprints. The authors declare no competing interests.

References

1. The new drugs of 2019. *C&EN Glob. Enterp.* **98**, 30–36 (2020).
2. Afanasyev, O. I., Kuchuk, E., Usanov, D. L. & Chusov, D. Reductive Amination in the Synthesis of Pharmaceuticals. *Chem. Rev.* **119**, 11857–11911 (2019).
3. Marshall, J. R. *et al.* Screening and characterization of a diverse panel of metagenomic imine reductases for biocatalytic reductive amination. *Nat. Chem.* **13**, 140–148 (2021).
4. Blakemore, D. C. *et al.* Organic synthesis provides opportunities to transform drug discovery. *Nat. Chem.* **10**, 383–394 (2018).
5. Roughley, S. D. & Jordan, A. M. The medicinal chemist's toolbox: An analysis of reactions used in the pursuit of drug candidates. *Journal of Medicinal Chemistry* (2011). doi:10.1021/jm200187y
6. Yasukawa, T., Masuda, R. & Kobayashi, S. Development of heterogeneous catalyst systems for the continuous synthesis of chiral amines via asymmetric hydrogenation. *Nat. Catal.* **2**, 1088–1092 (2019).
7. Wu, Z. *et al.* Secondary amines as coupling partners in direct catalytic asymmetric reductive amination. *Chem. Sci.* **10**, 4509–4514 (2019).

8. Skrypai, V., Varjosaari, S. E., Azam, F., Gilbert, T. M. & Adler, M. J. Chiral Brønsted Acid-Catalyzed Metal-Free Asymmetric Direct Reductive Amination Using 1-Hydrosilatrane. *J. Org. Chem.* **84**, 5021–5026 (2019).
9. Aleku, G. A. *et al.* A reductive aminase from Aspergillus oryzae. *Nat. Chem.* **9**, 961–969 (2017).
10. Mayol, O. *et al.* A family of native amine dehydrogenases for the asymmetric reductive amination of ketones. *Nat. Catal.* **2**, 324–333 (2019).
11. Yang, Y., Cho, I., Qi, X., Liu, P. & Arnold, F. H. An enzymatic platform for the asymmetric amination of primary, secondary and tertiary C(sp 3)–H bonds. *Nat. Chem.* **11**, 987–993 (2019).
12. Li, T. *et al.* Efficient, Chemoenzymatic Process for Manufacture of the Boceprevir Bicyclic [3.1.0]Proline Intermediate Based on Amine Oxidase-Catalyzed Desymmetrization. *J. Am. Chem. Soc.* **134**, 6467–6472 (2012).
13. Zhou, J. & List, B. Organocatalytic Asymmetric Reaction Cascade to Substituted Cyclohexylamines. *J. Am. Chem. Soc.* **129**, 7498–7499 (2007).
14. Monti, D. *et al.* Cascade Coupling of Ene-Reductases and ω-Transaminases for the Stereoselective Synthesis of Diastereomerically Enriched Amines. *ChemCatChem* **7**, 3106–3109 (2015).
15. France, S. P., Hepworth, L. J., Turner, N. J. & Flitsch, S. L. Constructing Biocatalytic Cascades: In Vitro and in Vivo Approaches to de Novo Multi-Enzyme Pathways. *ACS Catal.* **7**, 710–724 (2017).
16. Huffman, M. A. *et al.* Design of an in vitro biocatalytic cascade for the manufacture of islatravir. *Science.* **366**, 1255–1259 (2019).
17. Toogood, H. S. & Scrutton, N. S. Discovery, Characterization, Engineering, and Applications of Ene-Reductases for Industrial Biocatalysis. *ACS Catal.* **8**, 3532–3549 (2018).
18. Roth, S., Kilgore, M. B., Kutchan, T. M. & Müller, M. Exploiting the Catalytic Diversity of Short-Chain Dehydrogenases/Reductases: Versatile Enzymes from Plants with Extended Imine Substrate Scope. *ChemBioChem* **19**, 1849–1852 (2018).
19. Hyslop, J. F. *et al.* Biocatalytic Synthesis of Chiral *N*-Functionalized Amino Acids. *Angew. Chemie* **130**, 14017–14020 (2018).
20. Kato, Y., Yamada, H. & Asano, Y. Stereoselective synthesis of opine-type secondary amine carboxylic acids by a new enzyme opine dehydrogenase use of recombinant enzymes. *J. Mol. Catal. B Enzym.* **1**, 151–160 (1996).
21. Schober, M. *et al.* Chiral synthesis of LSD1 inhibitor GSK2879552 enabled by directed evolution of an imine reductase. *Nat. Catal.* **2**, 909–915 (2019).
22. Bornadel, A. *et al.* Technical Considerations for Scale-Up of Imine-Reductase-Catalyzed Reductive Amination: A Case Study. *Org. Process Res. Dev.* **23**, 1262–1268 (2019).
23. Hussain, S. *et al.* An (R)-Imine Reductase Biocatalyst for the Asymmetric Reduction of Cyclic Imines. *ChemCatChem* **7**, 579–583 (2015).
24. Yao, P., Xu, Z., Yu, S., Wu, Q. & Zhu, D. Imine Reductase-Catalyzed Enantioselective Reduction of Bulky α,β-Unsaturated Imines en Route to a Pharmaceutically Important Morphinan Skeleton. *Adv. Synth.*

Catal. **361**, 556–561 (2019).

25. Mitsukura, K. *et al.* Purification and Characterization of a Novel (R)-Imine Reductase from Streptomyces sp. GF3587. *Biosci. Biotechnol. Biochem.* **75**, 1778–1782 (2011).
26. Lenz, M. *et al.* Asymmetric Ketone Reduction by Imine Reductases. *ChemBioChem* **18**, 253–256 (2017).
27. Thorpe, T. W. *et al.* One-Pot Biocatalytic Cascade Reduction of Cyclic Enimines for the Preparation of Diastereomerically Enriched N -Heterocycles. *J. Am. Chem. Soc.* **141**, 19208–19213 (2019).
28. Steiningerova, L. *et al.* Different Reaction Specificities of F420 H2-Dependent Reductases Facilitate Pyrrolobenzodiazepines and Lincomycin To Fit Their Biological Targets. *J. Am. Chem. Soc.* **142**, 3440–3448 (2020).
29. Trenti, F., Yamamoto K., Hong B., Paetz C., Nakamura Y., & O'Connor S. E. Early and Late Steps of Quinine Biosynthesis. *Org. Lett.* **23** 1793–1797 (2021).
30. Mitsukura, K., Suzuki, M., Tada, K., Yoshida, T. & Nagasawa, T. Asymmetric synthesis of chiral cyclic amine from cyclic imine by bacterial whole-cell catalyst of enantioselective imine reductase. *Org. Biomol. Chem.* **8**, 4533 (2010).
31. France, S. P. *et al.* Identification of Novel Bacterial Members of the Imine Reductase Enzyme Family that Perform Reductive Amination. *ChemCatChem* **10**, 510–514 (2018).
32. Mangas-Sanchez, J. *et al.* Asymmetric synthesis of primary amines catalyzed by thermotolerant fungal reductive aminases. *Chem. Sci.* **11**, 5052–5057 (2020).
33. Montgomery, S. L. *et al.* Characterization of imine reductases in reductive amination for the exploration of structure-activity relationships. *Sci. Adv.* **6**, eaay9320 (2020).
34. Ouellet, S. G., Walji, A. M. & Macmillan, D. W. C. Enantioselective Organocatalytic Transfer Hydrogenation Reactions using Hantzsch Esters. *Acc. Chem. Res.* **40**, 1327–1339 (2007).
35. Rodríguez-Mata, M. *et al.* Structure and Activity of NADPH-Dependent Reductase Q1EQE0 from Streptomyces kanamyceticus, which Catalyses the R-Selective Reduction of an Imine Substrate. *ChemBioChem* **14**, 1372–1379 (2013).
36. Holm, L. Benchmarking fold detection by DaliLite v.5. *Bioinformatics* **35**, 5326–5327 (2019).
37. Lenz, M. *et al.* New imine-reducing enzymes from β-hydroxyacid dehydrogenases by single amino acid substitutions. *Protein Eng. Des. Sel.* **31**, 109–120 (2018).
38. Huber, T. *et al.* Direct Reductive Amination of Ketones: Structure and Activity of *S* -Selective Imine Reductases from *Streptomyces*. *ChemCatChem* **6**, 2248–2252 (2014).
39. Man, H. *et al.* Structure, activity and stereoselectivity of NADPH-dependent oxidoreductases catalysing the S-selective reduction of the imine substrate 2-methylpyrroline. *ChemBioChem* **16**, 1052–1059 (2015).
40. Aleku, G. A. *et al.* Stereoselectivity and Structural Characterization of an Imine Reductase (IRED) from *Amycolatopsis orientalis*. *ACS Catal.* **6**, 3880–3889 (2016).

41. Trott, O. & Olson, A. J. AutoDock Vina: Improving the speed and accuracy of docking with a new scoring function, efficient optimization, and multithreading. *J. Comput. Chem.* (2009). doi:10.1002/jcc.21334

Figures

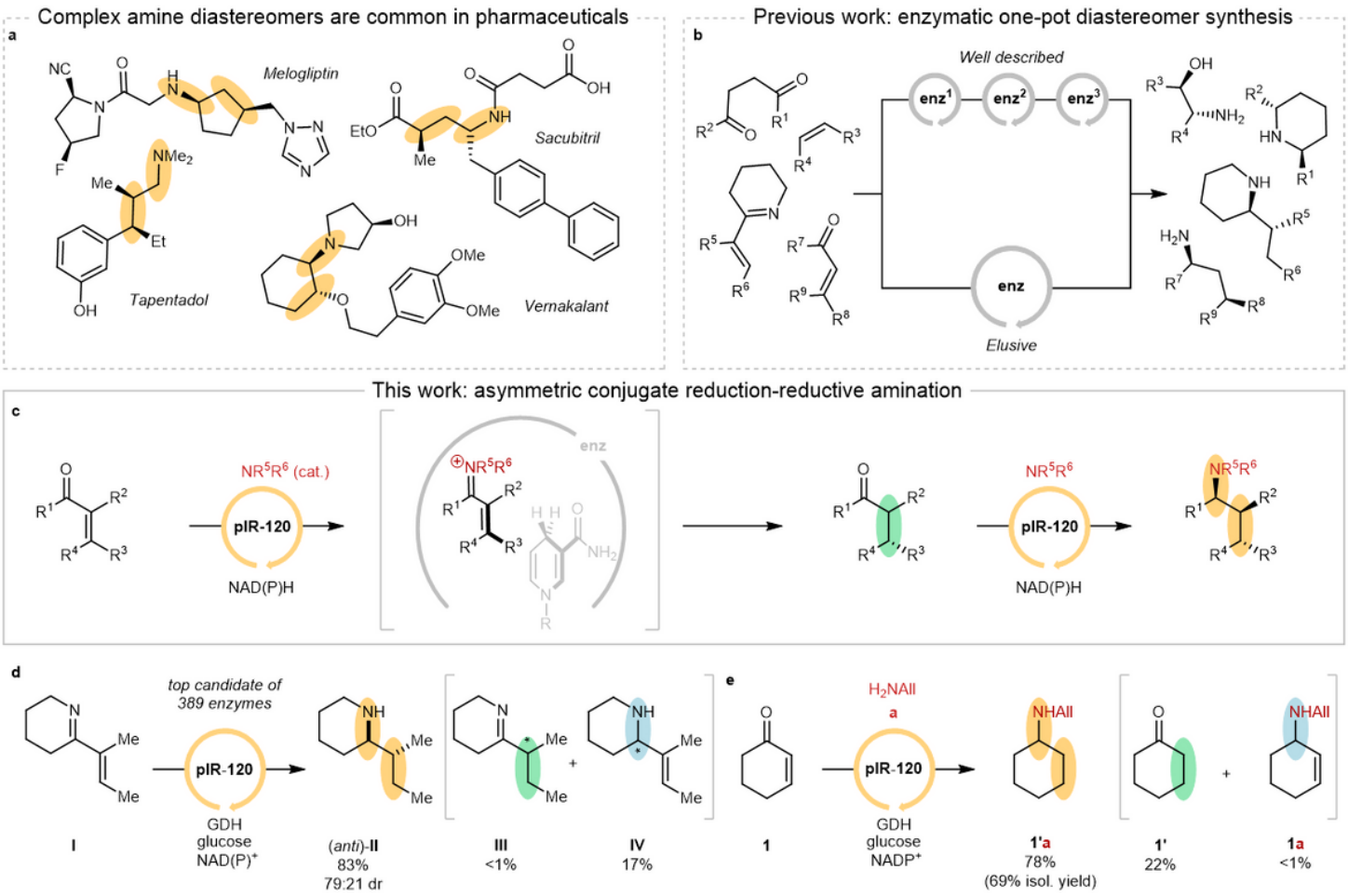

Figure 1

Enantioenriched amine diastereomers and enzymatic one-pot strategies for their synthesis. a: enantioenriched amine diastereomers are common in APIs, b: one-pot strategies for the enzymatic synthesis of stereoenriched amine diastereomers, c: our approach for developing a single enzyme-catalysed conjugate reduction-reductive amination (CR-RA) to prepare enantioenriched amine diastereomers, d: identification of C=C and C=N reducing pIR-120 by screening 389 putative IREDs, e: optimised reaction conditions for pIR-120-catalysed CR-RA, see Supplementary Information for full details.

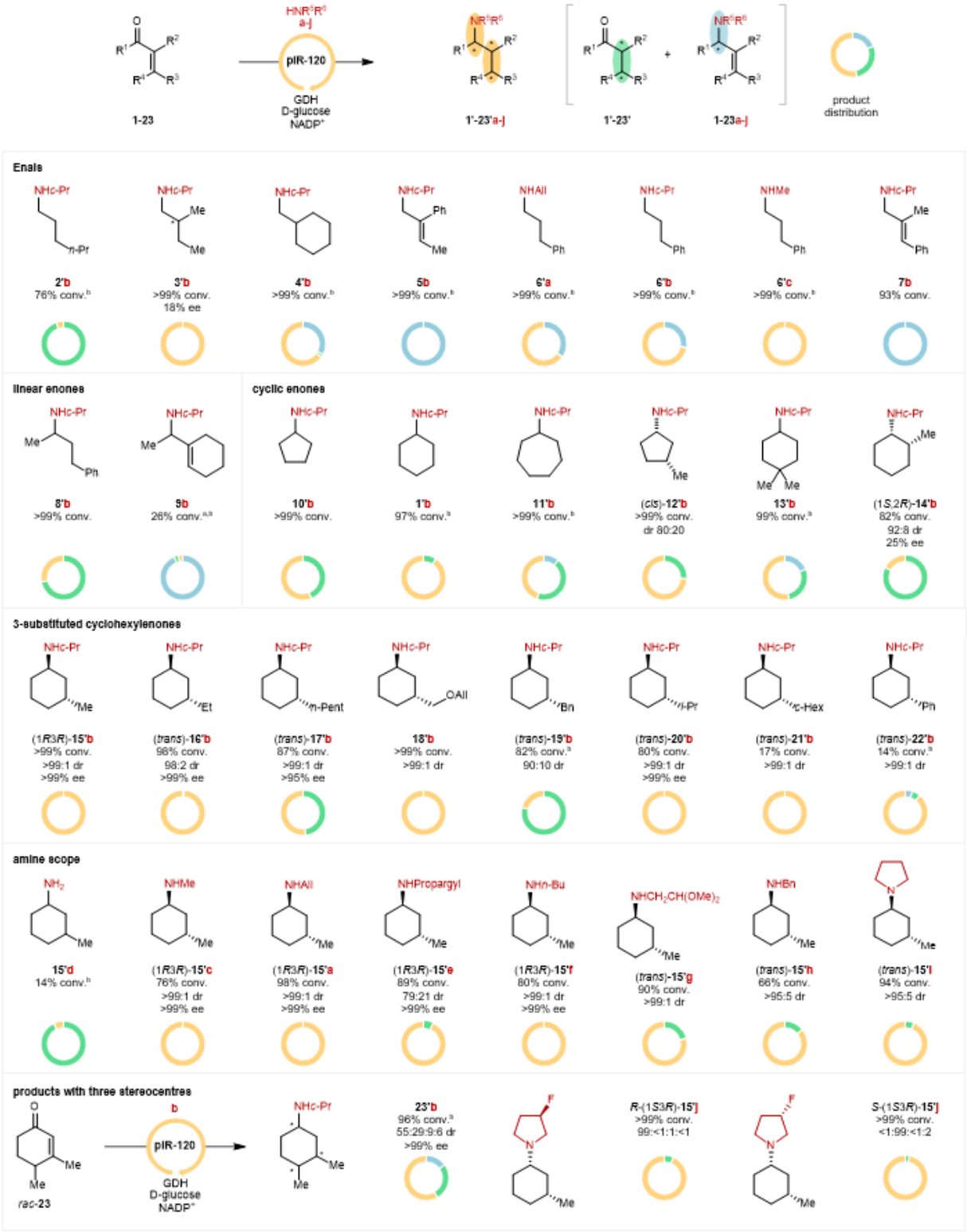

Figure 2

Substrate scope of pIR-120-catalysed CR-RA. Major RA product is drawn, product distribution is illustrated by the donut chart, % conversion = ∑(area% of CR and RA products). a non-enzymatic aza-conjugate addition product observed, b certain components determined by analogy based on the GC-MS spectrum, see Supplementary Table S2 for further details.

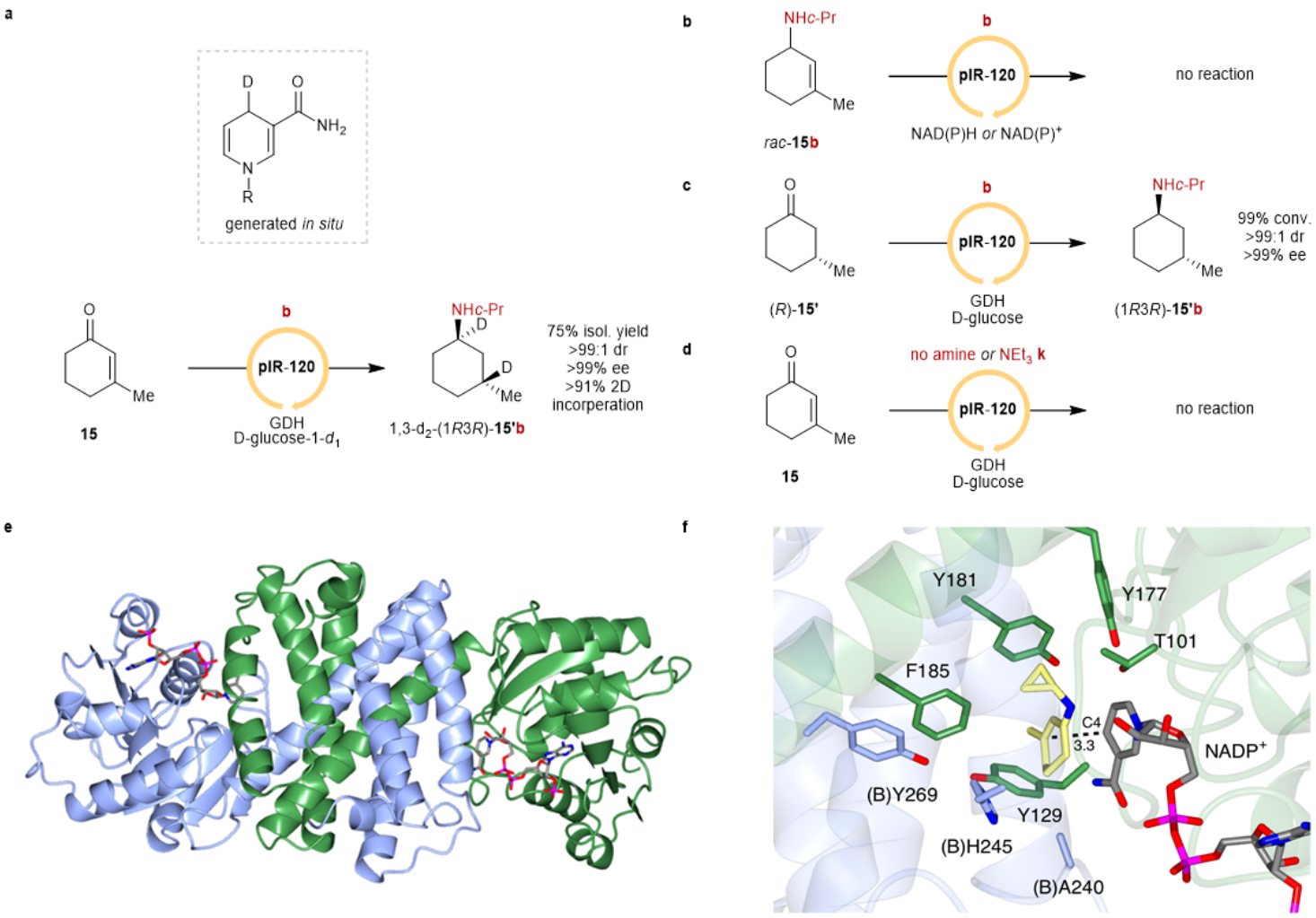

Figure 3

Mechanistic and structural studies. a: deuterium labelling experiment, b and c: isolated reactions of potential CR-RA pathway intermediates, d: amine donor control experiment, e: Structure of pIR-120 dimer in ribbon format with monomers A and B shown in green and blue respectively, f: Active site of pIR-120 in complex with NADP+. Side chains of monomers A and B are shown in cylinder format with carbon atoms in green and blue respectively. The structure has been used to model the enimine ligand (the condensation product of 15' and b), shown with carbon atoms in yellow. The distance between these atoms is given in Ångstroms.

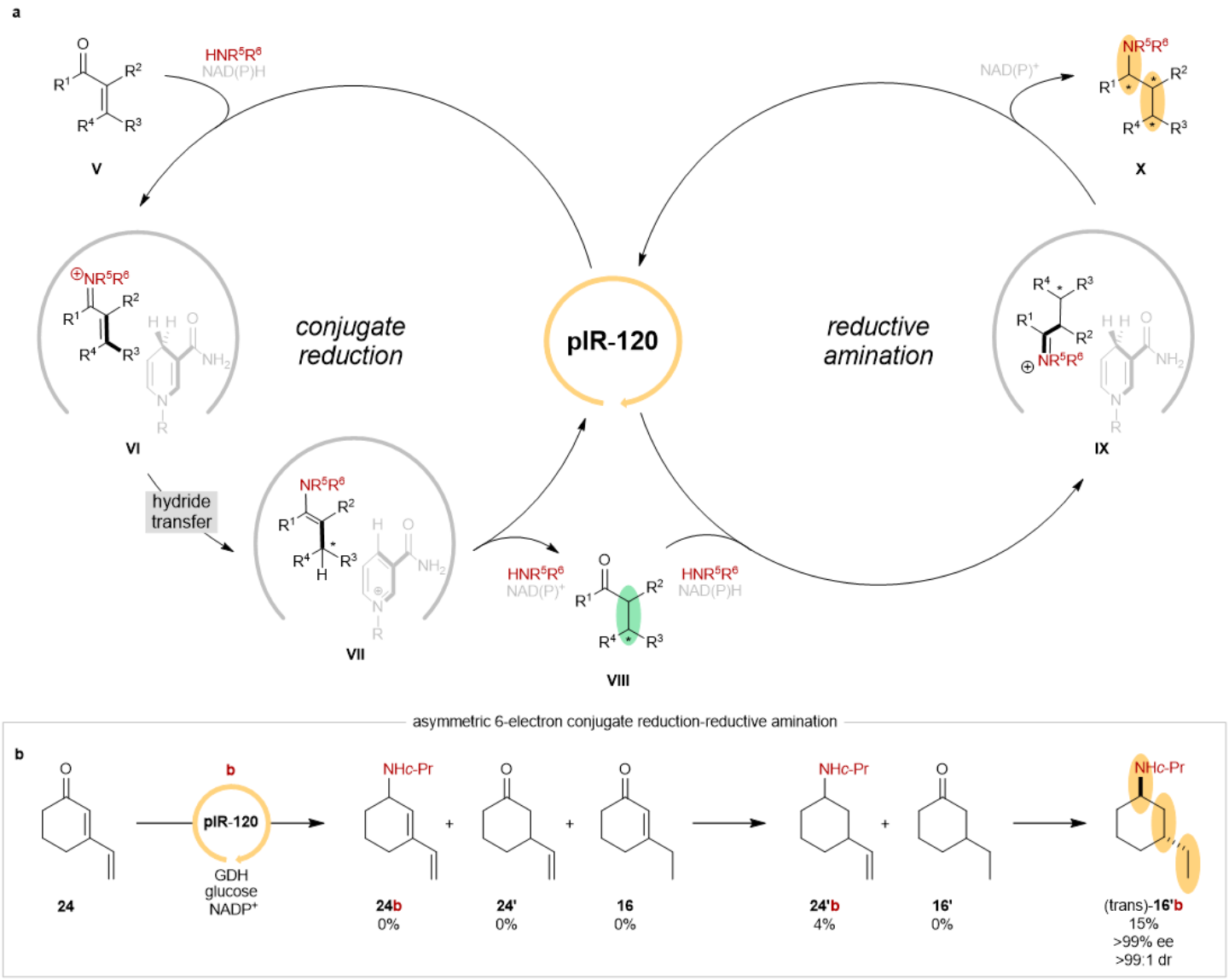

Figure 4

Proposed catalytic cycle of productive pIR-120 conjugate reduction-reductive amination (CR-RA) and extension to 6-electron CR-RA. a: schematic of the proposed catalytic cycles for pIR-120-catalysed CR and RA demonstrating the productive CR-RA reaction of α,β-unsaturated carbonyls and amines, b: example of 6-electron enzymatic CR-RA catalysed by pIR-120 only, by-product formation observed, see Supplementary Information for further details.

Supplementary Files

This is a list of supplementary files associated with this preprint. Click to download.

- D1292109198valreportfullP1.pdf
- pIR120SI.pdf

- ExtendedDataFigures.docx